Numerical study on excess pore pressure response of Champlain Sea Clay under 1-D constant rate of strain loading

Cong Shi
Department of Civil Engineering - Ryerson University, Toronto, Canada
Tareq Salloum
Ontario Power Generation, Niagara-on-the-Lake, Canada

ABSTRACT
This paper presents numerical simulations of constant rate of strain (CRS) consolidation tests performed on undisturbed Champlain Sea Clay samples to investigate the influence of strain rate, soil compressibility and permeability on the excess pore pressure response. The soil's compressibility parameters were first obtained from interpretation of the CRS tests results and then calibrated by the test simulation using a material model considering destructuration. The modeling reveals that the surge in excess pore pressure Δu_b observed at early stage of normal consolidation is mainly related to the dramatic compressibility increase of soil when effective stress over passes the pre-consolidation pressure, also known as destructuration. The parametric studies provide further evidence that higher soil compressibility and strain rate would result in higher excess pore pressure. A non-linear Δu_b relationship with strain ε is observed from the test data and confirmed by numerical simulations. The slope C_k describing the permeability relationship with void ratio is another factor causing noticeable difference in excess pore pressure development in numerical modeling. Lower C_k would results in higher Δu_b and more significant non-linear $\Delta u_b \sim \varepsilon$ relationship.

RÉSUMÉ
Cet article présente des simulations numériques de tests de consolidation à vitesse constante de déformation (CRS) effectués sur des échantillons d'argile de Champlain non perturbés pour étudier l'influence de la vitesse de déformation, de la compressibilité du sol et de la perméabilité sur la réponse interstitielle. Les paramètres de compressibilité du sol ont d'abord été obtenus à partir de l'interprétation des résultats des tests CRS puis calibrés par la simulation d'essai à l'aide d'un modèle matériel tenant compte de la déstructuration. La modélisation révèle que l'augmentation de la pression interstitielle Δu_b observée au début de la consolidation normale est principalement liée à l'augmentation considérable de la compressibilité du sol lorsque la contrainte effective dépasse la pression de pré-consolidation, également appelée déstructuration. Les études paramétriques fournissent une preuve supplémentaire qu'une compressibilité et une vitesse de déformation du sol plus élevées entraîneraient une pression interstitielle en excès plus élevée. Une relation Δu_b non linéaire avec souche ε est observée à partir des données de test et confirmée par des simulations numériques. La pente C_k décrivant la relation de perméabilité avec le taux de vide est un autre facteur causant une différence notable dans le développement de la pression interstitielle en excès dans la modélisation numérique. Une valeur inférieure de C_k entraînerait une plus grande valeur de Δu_b et une relation $\Delta u_b \sim$ ε non linéaire plus importante.

1 INTRODUCTION

Constant rate of strain (CRS) consolidation tests are widely used nowadays as an alternative of incremental loading (IL) consolidation tests in that (1), much higher density of data points available and faster test speed, (2) controlled strain rate at both loading and unloading stages, and (3) back pressure applied for sample saturation (Wissa 1971).

During the loading stage of a CRS test, one side of the soil sample is drained, while another side is undrained where excess pore pressure is generated. The amount of excess pore pressure should be controlled by the allowable strain rate applied. The ratio of base excess pore pressure to total vertical stress u_b/σ_v has been used by many researchers (Larsson and Sallfors 1985, Sheahan and Watters 1997, ASTM 2008) as a criterion to determine the allowable strain rate for tests, but the suggested values fall into a wide range from 0.03 to 0.7 depending upon soil types. Based on the CRS test results, Ahmadi (2014) reported that the excess pore pressure in non-sensitive clays is approximately linearly correlated to the strain regardless of the plasticity of the clays. However, the experimental study on a sensitive clay in Eastern Canada, involving both CRS tests and constant-gradient tests, demonstrated a non-linear relationship between excess pore pressure and strain (Silvestri 1986). The reason is that the development of excess pore pressure is coherently influenced by a number of factors, including strain rate, soil plasticity, organic content, soil compressibility and permeability (Reddy 2015). Additional efforts are still needed to investigate the influences of these factors on the excess pore pressure to arrive at the allowable strain rates suitable to different types of soils. The finite element method (FEM) provides an accessible way to approach this problem by conducting parametric study on the soil properties involved.

This paper presents a series of numerical simulations of CRS tests performed on the undisturbed Champlain Sea Clay in Eastern Canada to study the influences of strain rate, soil compressibility, and permeability on the excess pore water pressure induced during the tests.

2 PHYSICAL PROPERTY OF THE SOIL

The soil used in this study was Champlain Sea Clay collected near the Town of Arnprior in northern Ontario, Canada. The investigation was to study the geotechnical properties of the marine clay foundation of an embankment. The embankment was built with 9.7 m thick berm underlain by Champlain Sea Clay. The undisturbed samples with inner diameter and height of 200 mm and 220 mm were extruded using a Laval sampler. The color of clay was mainly grey, varying from dark gray, greenish gray and gray. Most samples were found to be homogeneous with firm consistency. Fish shells were noticed sometimes in the sample which was an indicative of its marine nature. Three depths (11.36, 12.00 and 25.20 m) of the sample are used in this study. The depths here are specified from the berm surface at EL:97.32 m. See Table 1 for the detailed properties.

Table 1. Properties of the test material

Depth (m)	11.36-25.2
Bulk density (kg/m^3)	1528-1655
Water content (%)	73.3 – 80.3
Liquid limit (%)	71.1-77.2
Plasticity index	46.6-50.0
Specific gravity	2.74-2.78
Undrained shear strength (kPa)	37-50
Sensitivity	12.9-13.4
Salinity (g/L)	3.9-5.9

3 TEST SETUP

A series of CRS tests were conducted on the undisturbed clay samples according to ASTM standard D4186-06 (ASTM 2008). The soil sample was first trimmed carefully into a CRS ring with a diameter of 6.35 cm and a height of 2.54 cm. A porous stone was placed on the top for the consolidation drainage, while the bottom was kept undrained. After the CRS ring was put into the cell, a back pressure of about 350 kPa was applied for about 20 hours to saturate the sample. Then, an axial load was applied from the top allowing the sample to deform at the assigned constant strain rate. The force reaction and excess pore pressure response were captured by the load cell and pore pressure sensor throughout the test. The strain rate of 0.5 to 1 %/hr was selected to ensure the ratio u_b/σ_v within 3 % to 15 % during the tests.

Three CRS tests were selected to verify the numerical model. See Table 2 for the test details. The test results are shown in Figure 3 along with simulations.

Table 2. Properties of the test material

Test No	Depth (m)	Strain rate (%/hr)	Maximum stress reached (kPa)
1	11.36	1	1900
2	12	0.5	1900
3	25.2	0.5	2400

4 MATERIAL MODEL

The destructuration behavior attributed to plastic straining is a crucial feature of this marine clay, understood as a collapsed segment of the compression part immediately after pre-consolidation pressure shown in Figure 1.

The soil model (MEVP) employed in this paper was developed on the elasto-viscoplastic (EVP) framework by (Yin 2002). The model was later strengthened with destructuration behavior and anisotropy by (Koskinen 2002). The focus of this study is on the destructuration feature and the anisotropy is not considered in this study.

The bonding of MEVP model is described as:

$$\sigma_p' = (1 + \chi_0)\sigma_{pi}' \quad [1]$$

where χ_0 is the initial bonding. σ_p' is the pre-consolidation pressure, understood as the static yield surface, and σ_{pi}' is the intrinsic yield surface related to the remolded sample shown in Figure 1.

The bonding destructuration due to the plastic straining is governed by:

$$d\chi = -\xi \cdot \chi \cdot (\left|d\varepsilon_v^{vp}\right| + \xi_d \cdot d\varepsilon_d^{vp}) \quad [2]$$

where χ is the amount of particle bonding, which decreases with plastic straining and finally coincide with the intrinsic line obtained from remolded clay. λ_i is the slope of intrinsic compression line. ξ is the absolute effectiveness of destructuration hardening, $\xi_d$the relative effectiveness of destructuration hardening. $d\varepsilon_v^{vp}$ is the inelastic volumetric strain, and $d\varepsilon_d^{vp}$ is the inelastic deviatoric strain.

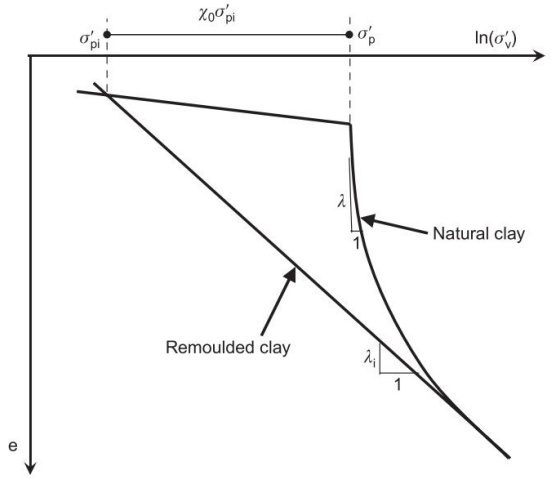

Figure 1. Definition of destructuration of structural marine clay (Karstunen and Yin 2010)

5 MODEL DESCRIPTION

The circular 1-D CRS sample was modeled as an axisymmetric problem in 2D Plaxis software (Plaxis 2006). The sample size, boundary conditions and strain rates of the simulations were identical to the tests performed.

The parameters listed in Table 3 were obtained from the interpretation of CRS test results. Parameters such as initial void ratio e_0, recompression index κ and pre-consolidation pressure P_c' can be easily interpreted from the $e-logp'$. Note that κ is analogous to C_s which is defined in the $e-logp'$ scale, but κ is defined in the $e-lnp'$ scale. Therefore, $C_s = 2.3\kappa$ can be used to convert C_s to κ. Similarly, $C_c = 2.3\lambda$ can be used to convert C_c to λ. Figure 2 (a) presents how the destructuration parameters λ_i and χ_0 were interpreted, using 25.2 m test result as an example. ξ and ξ_d need to be calibrated by the trial simulation to arrive at the best fitting of the compression curve. The calibrated ξ and ξ_d can be found in Table 3. Note that ξ_d is a less sensitive parameter and $\xi_d = 0.2\sim0.3$ are usually taken for analysis (Yin 2011). Figure 2 (b) shows the definition of permeability parameters k_0 and C_k from the $e\sim logk$ graph attained from the tests. $C_k = \Delta e/\Delta logk$ defined here is to describe the slope of permeability in a logarithm scale with void ratio in the normally consolidated range. k_0 is adjusted from the line as the permeability at the initial void ratio. For the samples tested at other depths, C_k is found falling into the range of $C_k = 0.5\sim0.55e_0$.

The secondary consolidation index C_α and critical state stress ratio M came from the long-term oedometer tests and triaxial compression tests conducted at similar depths and the results are not shown in this paper. The Soft Soil Creep model (SSC) is also used here for comparison with MEVP model. Note that SSC model is not able to consider destructuration and employs the linear slope λ similar to Modified Cam Clay. Here for simplicity, λ for SSC model is adjusted as the average slope between $1P_c'$ and $5P_c'$.

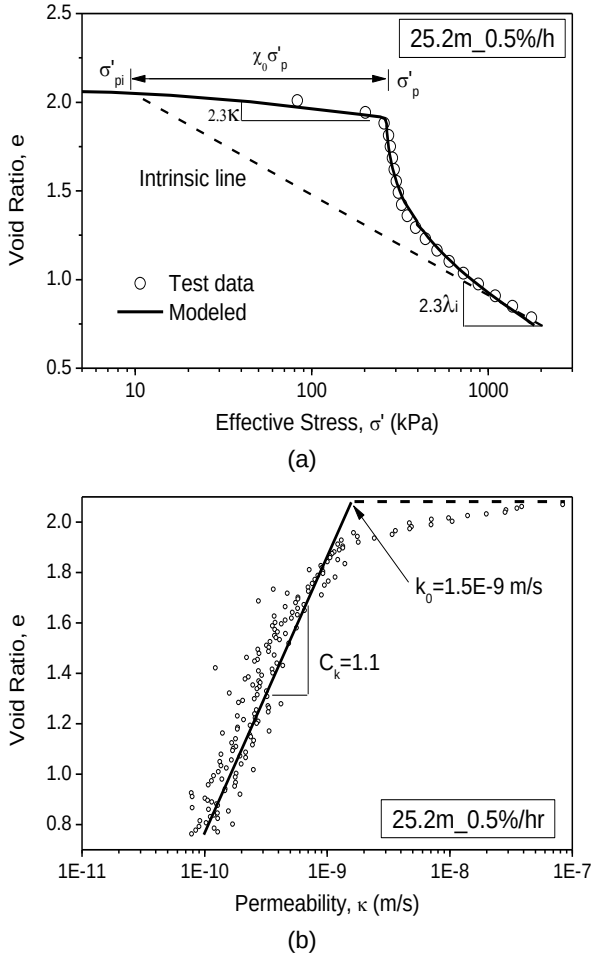

Figure 2. Interpretation of model parameters from test results

Table 3 Parameters for consolidation and shear strength properties

Depth	e_0	κ	ν	P_c'	k_0	C_k	C_α	M	SSC λ^1	MEVP λ_i	MEVP χ_0	MEVP ξ	MEVP ξ_d
25.2m	2.07	0.03	0.3	250kPa	1.5e-9 m/s	1.1	0.06	1.2	0.64	0.5	18	11.5	0.2
12m	2.00	0.03	0.3	140kPa	1.5e-9 m/s	1.1	0.06	1.2	0.44	0.35	24	13	0.2
11.36m	2.05	0.03	0.3	121kPa	1.5e-9 m/s	1.1	0.06	1.2	0.44	0.35	20	12.5	0.2

[1]For SSC model, λ is adjusted as the average slope between $1P_c'$ and $5P_c'$ due to the nonlinearity of compression curve. For MEVP model λ_i from the intrinsic line is used instead.

6 TEST AND MODELING RESULTS

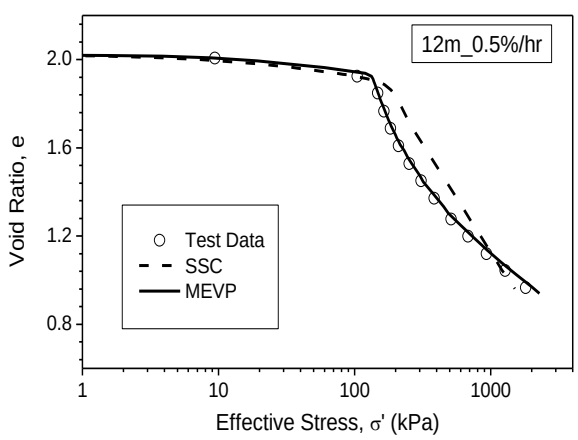

(a)

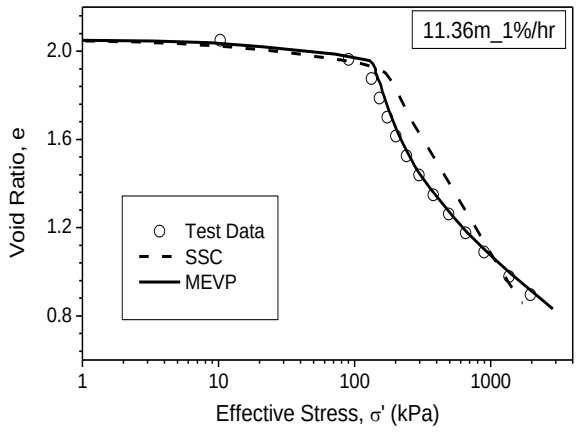

(b)

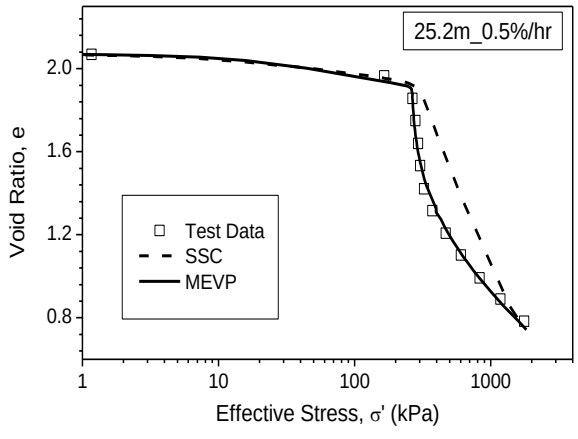

(c)

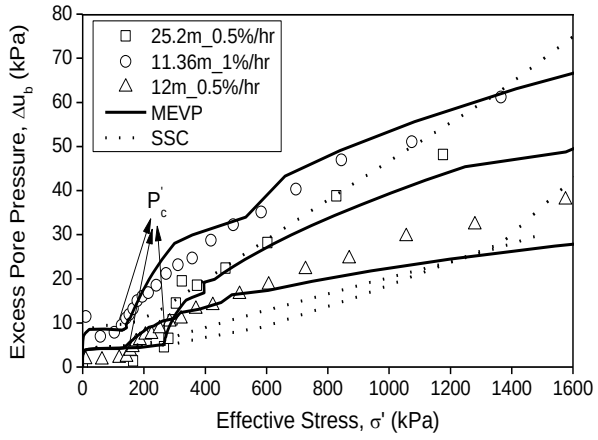

(d)

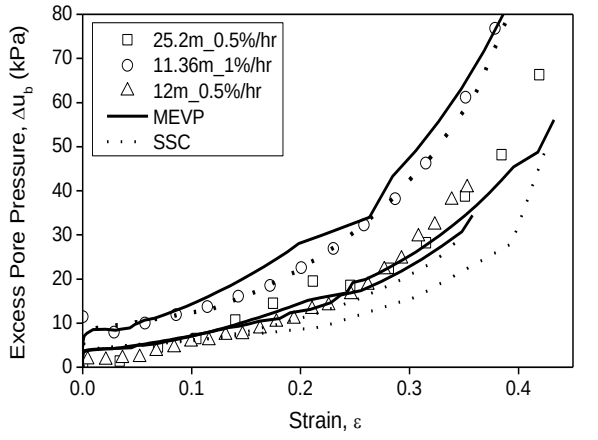

(e)

Figure 3. Numerical simulation compared with test data

Figure 3(a) to (e) demonstrate the simulated CRS tests using SSC and MEVP model. The simulated e-logp' curves are compared with the laboratory results in Figure 3(a) to (c).

It can be seen that MEVP model apparently better captures the nonlinear compression curve of the undisturbed marine clay than SSC model. Both destructuration (collapsed segment right after pre-consolidation pressure) and restructuration (flatter segment at the end) are simulated by the MEVP model.

The excessive pore pressure at base Δu_b has been measured during the course of CRS loading, and the development is also compared with the numerical results in Figure 3(d) to (e). The measured pore pressure sees a tremendous jump when the effective stress passes the pre-consolidation. The MEVP model successfully captures this behavior compared to SSC model, indicating that the dramatic pore pressure increase is mainly due to the volume decrease related to destructuration. Δu_b's increase with ε reveals a non-linear fashion, and hence Δu_b increases faster with time assuming a constant strain rate applied.

7 PARAMETRIC STUDY

A series of numerical simulations are presented here to demonstrate the influences of strain rate, soil compressibility and permeability on the excess pore pressure response using MEVP model. The modeling result of 25.2 m_0.5%/hr is used here as the control group.

7.1 Strain rate

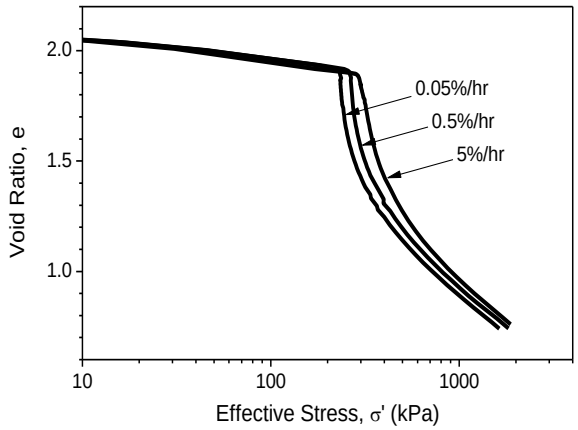

(a)

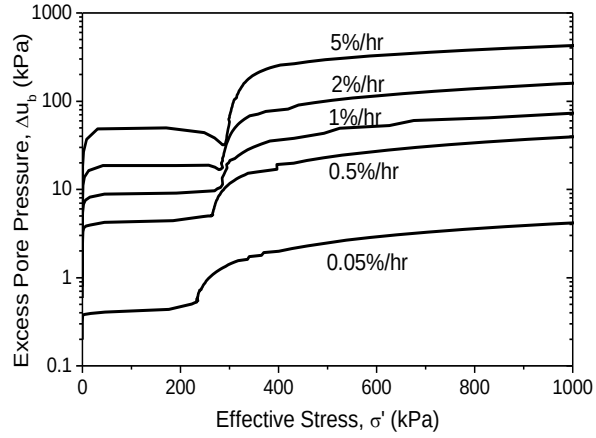

(b)

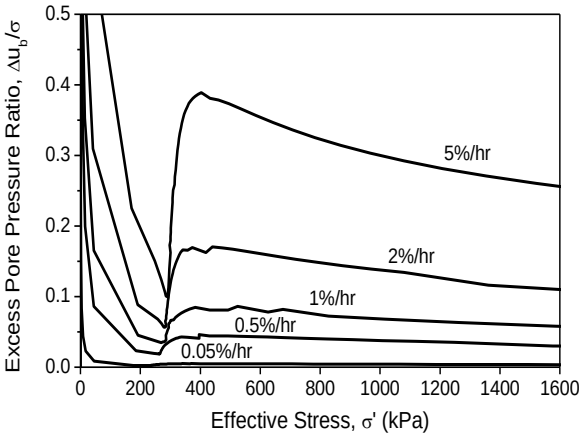

(c)

Figure 4. Strain rate effect on e-logp' curves and excess pore pressure

Five strain rates from 0.05%/hr to 5%/hr are applied to the sample, and their influences on e-logp' curves and excess pore pressure are shown in Figure 4 (a) to (c).

As expected, higher strain rates will lead to higher pre-consolidation pressures. The pre-consolidation pressure shown in Figure 4 (a) increases by 15% and 34% respectively compared to the 0.05%/hr case when the loading strain rate goes up to 0.5%/hr and 5%/hr. The increase in strain rate also results in higher excess pore pressure. Δu_b and u_b/σ_v ratio variation attributed to different strain rates are plotted in Figure 4 (b) and (c) respectively. For the 25.2 m depth sample studied here, the 5%/hr strain rate can be seen to cause u_b/σ_v to reach over 0.3, whereas 0.05%/hr hardly generates any pore pressure, see Figure 4 (c).

7.2 Soil compressibility

Figure 5 (a) and Figure 6 (a) present how the destructuration parameters are governed by two parameters: χ_0 and ξ. The increase of these two parameters will lead to steeper compression curves and hence higher compressibility of soil. Figure 5 (b) and Figure 6 (b) demonstrate that the increase in compressibility of soil will lead to higher excess pore pressure.

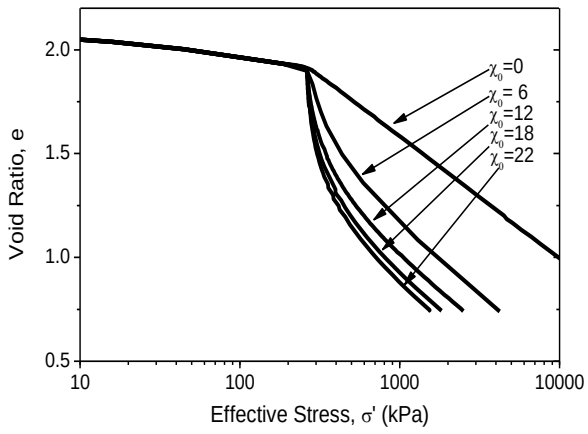

(a)

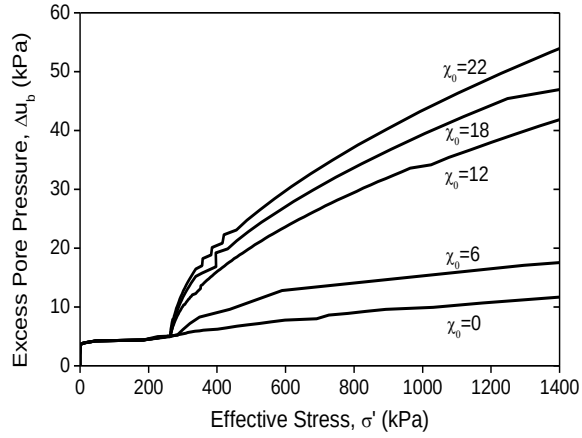

(b)

Figure 5. χ_0 effect on e-logp' curves and excess pore pressure

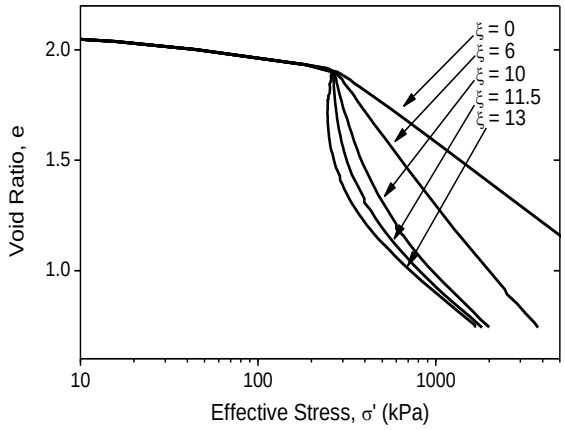

(a)

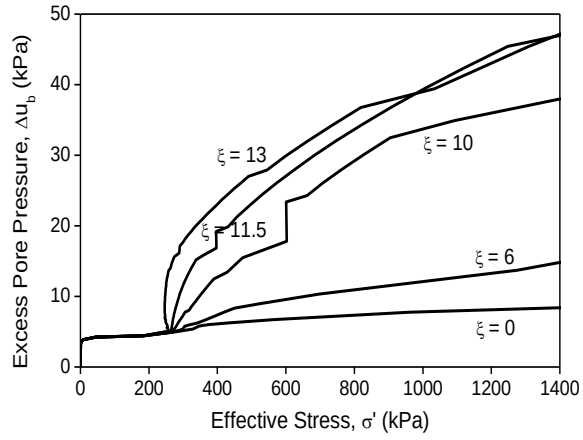

(b)

Figure 6. ξ effect on e-logp' curves and excess pore pressure

7.3 Permeability

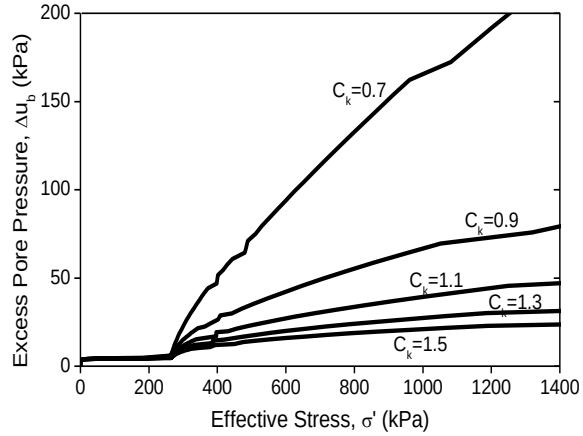

(a)

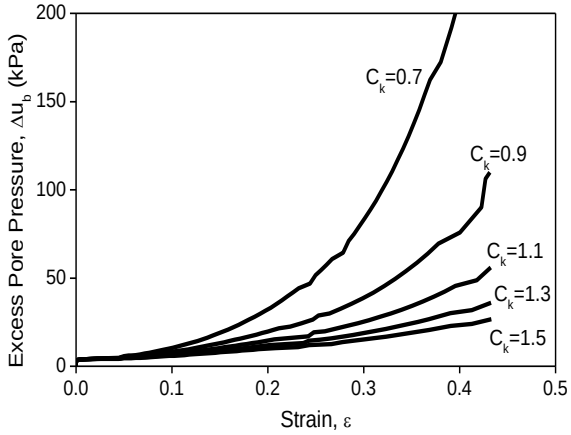

(b)

Figure 7. C_k effect on excess pore pressure

Figure 7 (a) shows that C_k is another factor that will make noticeable difference in pore pressure generation. A lower C_k, which results in a lower permeability given the same amount of void ratio change, can cause a higher excess pore pressure. The excess pore pressure rises from 40 kPa to 67 kPa at σ'=1000 kPa (approximately $4P_c'$) when C_k reduced from 1.1 to 0.9. Moreover, a significant non-linearity $\Delta u_b \sim \varepsilon$ relationship is noticed in Figure 7 (b) when C_k is decreased from the tested value of 1.1 to 0.7.

8 CONCLUSIONS

The good agreement between the CRS tests performed on the undisturbed Champlain Sea Clay and numerical simulations verifies the FEM model used in this study. The further parametric study based on 25.2 m test simulation as control group provides evidence that the excess pore pressure generated during the tests are influenced by a number of factors including strain rate, soil compressibility and permeability. The conclusions are listed as follows:

1.The surge in excess pore pressure noticed at early stage of normal consolidation, as revealed by numerical modeling, is mainly attributed to the significant compressibility increase of soil when effective stress overpasses the pre-consolidation pressure, also known as destructuration.

2. The parametric study on two destructuration parameter χ_0 and ξ further demonstrates that the higher the compressibility of soil, the higher the excess pore pressure given the same strain rate and soil permeability.

3. Both test and modeling results indicate a non-linear excess pore pressure Δu_b relationship with strain ε during the loading stage of CRS tests.

4. The parametric study confirms that higher strain rate will induce a higher excess pore pressure during CRS tests. The modeling of 25.2 m case shows that the strain rate of 5%/hr can cause the ratio of excess pore pressure to total vertical stress u_b/σ_v to reach 0.3, while the strain rate as low as 0.05%/hr yields almost no excess pore pressure.

5. C_k is also found causing noticeable difference in excess pore pressure development in numerical modeling.

Lower C_k assigned to soil is shown to result in higher Δu_b and a more significant non-linear $\Delta u_b \sim \varepsilon$ relationship.

9 ACKNOWLEDGEMENTS

The authors want to express gratitude to Ontario Power Generation and Mitacs for the technical and financial support. Special thanks to Dr.Yin Jian-Hua of The Hong Kong Polytechnic University for sharing the MEVP soil model.

10 REFERENCES

Ahmadi, H., Rahimi, H. and Soroush, A. et al. (2014). Experimental research on variation of pore pressure in constant rate of strain consolidation test. Acta Geotechnica, 47-57.

ASTM. (2008). Standard test method for one-dimensional consolidation properties of soils using controlled-strain loading. *ASTM standard D4186-06. American Society of Testing Materials*, 520-533.

Karstunen, M. and Yin, Z. (2010). Modelling time-dependent behavior of Murro test embankment. *Geotechnique*, 735-749.

Koskinen, M., Karstunen, M. and Wheeler, S. J. (2002). Modelling destructuration and anisotropy of a natural soft clay. *Numerical Methods of Geotechnial Engineering*, (pp. 11-19). Paris.

Larsson, R. and Sallfors, G. (1985). Automatic continuous consolidation testing in Sweden. *In Consolidation of soils: testing and evaluation, Proceedings of the ASTM Committee D-18 Symposium on Soil and Rock*, (pp. 299-328). Orlando.

Plaxis (2015). *Reference manual V8*. Delft, The Netherlands: Plaxis BV

Reddy, B., Sahu, R. and Ghosh, S. (2015). Constant rate of strain consolidation of organic clay: in Kolkata region. *International Journal of Geotechnical Engineering*, 471-482.

Sheahan, T.C., and Watters, P.J. (1997). Experimental verification of CRS consolidation theory. *Jounral of Geotechnical and Geoenvironmental Engineering*, 430-437.

Silvestri, V. et al. (1986). Constrolled-strain, controlled-gradient, and standard consolidation testing of sensitive clays. *Testing and Evaluation. ASTM STP 892*, 433-450.

Wissa, A. E. Z., Christian, J. T., Davis, E. H. and Heigerg, S. (1971). Consolidation at constant rate of strain. *Canadian Geotechnical Journal*, 18-26.

Yin, J., Zhu, J. and Graham, J. (2002). A new elastic viscoplastic model for time dependent behavior of normally and overconsolidated clays: theory and verification. *Canadian Geotechnical Journal*, 157-173.

Yin. Z, Karstuen. M, Chang. C et al. (2011). Modeling time-dependent behavior of soft sensitive clay. *Journal of geotechnical and geoenvironmental engineering*, 1103-1113.